Interannual Variability of Deep-Water Formation in the Northwestern Mediterranean

C. MERTENS AND F. SCHOTT

Institut für Meereskunde, Universität Kiel, Kiel, Germany

(Manuscript received 1 April 1997, in final form 18 August 1997)

ABSTRACT

In the Gulf of Lions, observations of deep convection have been sporadically carried out over the past three decades, showing significant interannual variability of convection activity. As long time series of meteorological observations of the region are available from coastal stations, heat flux time series for the Gulf of Lions for the individual winters from 1969 to 1994 are derived by calibrating these observations against direct measurements obtained over the convection site. These heat fluxes are also compared against heat fluxes obtained by the French PERIDOT weather model for the winter of 1991/92. A Kraus–Turner one-dimensional mixed layer model is initialized by climatological mean temperature and salinity profiles and then driven by the heat flux time series of the individual years. Resulting convection depths are in satisfactory agreement with existing observational evidence, showing the dominance of interannual variability of local forcing on convection variability. The interannual variability of convection depth causes interannual variations in deep-water properties, and these are also compared with the hydrographic database.

1. Introduction

The Gulf of Lions in the northwestern Mediterranean is long known as a region where deep wintertime mixing and deep-water formation takes place. Facilitated by its relative ease of access the Gulf of Lions has been the subject of numerous studies, beginning with the classical MEDOC experiments (e.g., MEDOC Group 1970; Gascard 1973, 1978). The situation leading to deep convection in the Gulf of Lions has its basis in the cyclonic circulation, which consists of the Northern Current, flowing westward along the French coast, and its partial recirculation eastward at the southern boundary of the convection area (Millot 1987; Schott et al. 1996). This circulation leads to an uplifting of the isopycnals in an elongated dome off the southern French coast with a center of shallow surface mixed layer near 42°N, 5°E (Fig. 1).

The stratification is basically three layered: the top 150 m are occupied by modified Atlantic Water overlying a layer of warmer and saltier water, the Levantine Intermediate Water (LIW), which extends from 150 to 500 m. The deeper levels underneath are filled with weakly stratified Western Mediterranean Deep Water (WMDW). The reason for the susceptibility of the region to deep convection is that in winter cold and dry winds from two directions blow over the Gulf of Lions and over the shallowest part of that dome: the mistral from out of the Rhône Valley and the tramontana from the north side of the Pyrenees. These winds typically occur in strong bursts of a few days duration with high sensible and latent heat fluxes that can exceed total heat fluxes of 1000 W m^{-2} (e.g., Leaman and Schott 1991). When the forcing is strong enough during a winter season to erode the near-surface and intermediate-layer stability, the weakly stratified underwaters are exposed to the surface buoyancy flux and deep convection can occur.

In a typical convection season, the density gradient against the weakly stratified WMDW has nearly vanished around mid February. Buoyancy loss through strong wind events can now lead to mixing to great depths and homogenization of the water column in a *chimney* (Killworth 1976) of 50–100 km horizontal extent (Fig. 1). Early observations with rotating deep floats showed vertical motions of several centimeters per second at 800-m depth in the convection regime (Voorhis and Webb 1970). With the availability of measurements from moored acoustic Doppler current profilers (ADCPs), more detailed studies of small-scale processes during deep convection have become possible, showing downward motions of about 10 cm s^{-1} on horizontal scales less than 1 km and slow upward motions between those convective plumes (Schott and Leaman 1991). Subsequent tank experiments (Maxworthy and Narimousa 1994) and nonhydrostatic numerical modeling (Jones and Marshall 1993) supported the existence of such small-scale plumes. The overall effect of the plumes is to act as a strong mixing mechanism instead of causing a mean downdraft (Schott et al. 1994; Send

Corresponding author address: Christian Mertens, Institut für Meereskunde, Düsternbrooker Weg 20, 24105 Kiel, Germany.
E-mail: cmertens@ifm.uni-kiel.de

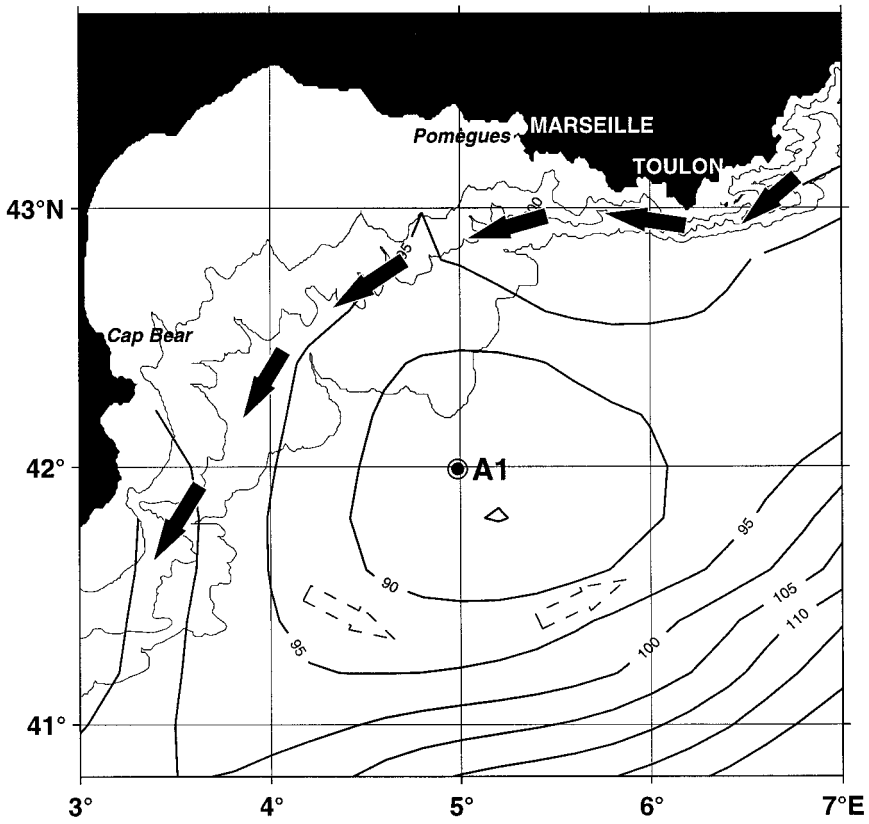

FIG. 1. Topography and circulation of the northwestern Mediterranean, and location of mooring A1 from the THETIS experiment. Also shown is the depth of the $\sigma_\theta = 28.8$ surface from climatological data.

and Marshall 1995), making the term chimney for a deep-mixed regime not quite representative. The role of convective plumes as just a large vertical eddy coefficient allows application of simple mixed layer models to study some of the integral effects of deep convection, like convection depth and water mass modification. The phase of convection today still least understood is that of the restratification and exchange with the surrounding stratified waters where instability eddies at the edge of the chimney play the key role. This phase, however, is not part of the present study.

Deep convection to intermediate or full ocean depths has been observed several times in the Gulf of Lions over the years since 1969, but there have also been years when a lack of deep convection was documented (e.g., Leaman 1994). Unlike the Labrador and Greenland Seas, where deep convection activity seems to be modulated at decadal timescales (Dickson et al. 1996), the convection variability in the northwestern Mediterranean seems to be of an interannual nature.

In the following we will investigate the interannual variability of convection depths by applying a one-dimensional Kraus–Turner-type model to typical preconditioning profiles of early winter and forcing it with the heat flux variations of each particular winter during the period from 1969 to 1994. Since no heat flux time series exist from over the convection region other than for the few instances of buoy or shipboard observations during convection experiments, we constructed time series from coastal meteorological stations by calibrating them against observations from over the site. Special emphasis will be on the winter 1991/92, when observational data are available from the THETIS experiment (Schott et al. 1996; THETIS Group 1994). Heat fluxes from the French weather prediction model PERIDOT (Leaman and Schott 1991) are evaluated here for this winter in comparison with shipboard observations and the calibrated coastal weather station data.

The interannual variability of convection results in interannual variability of water mass transformation. We present the mean hydrographic properties of the deep-mixed regime for the winters investigated and compare it with observational evidence where available.

2. The mixed layer model

The one-dimensional model used in the present study is conceptually similar to that of Kraus and Turner (1967) [see Niiler and Kraus (1977) for a review], but differs structurally. The temperature and salinity of the

mixed layer are adjusted three times within each time step of integration by heat and freshwater exchange at the surface, convective adjustment, and turbulent mixing. Similar formulations have been used to investigate convection in the Greenland Sea (Visbeck et al. 1995), the formation of Levantine Intermediate Water in the Eastern Mediterranean (Lascaratos et al. 1993), and to model the ocean's response to climatic change (Rahmstorf 1991).

The model is initialized using observed temperature and salinity profiles resolved into discrete depth layers. The surface fluxes of heat and freshwater are computed from meteorological observations using bulk parameterization formulas or prescribed by an external model, as described below. In case the stratification becomes unstable from surface cooling, convective mixing is performed through mixing subsequent layers until the density gradient at the base vanishes. Mixed layer deepening due to wind stirring is calculated from the turbulent kinetic energy equation:

$$-\frac{g}{2\rho_0}h\Delta\rho w_e = mU^3 + \frac{1}{2}nhB, \tag{1}$$

where w_e is the entrainment velocity of the mixed layer, h the mixed layer depth, $\Delta\rho$ the density step at the base of the mixed layer, U the wind speed, and B the combined thermal and haline surface buoyancy flux,

$$B = g\left[\frac{\alpha}{c_p\rho_0}Q - \beta S_0(E - P)\right]. \tag{2}$$

The empirical coefficients m, n account for the fractions of the wind mixing and buoyancy flux mixing energies that are used for mixed layer deepening. The wind mixing energy depends on the wind speed and is assumed to be dissipated exponentially with depth:

$$m = \rho_a c_D f_w \exp(-h/H_0), \tag{3}$$

where ρ_a is the air density, and c_D is the drag coefficient. The efficiency of wind mixing f_w is taken to be 1.5×10^{-3} with a dissipation scale $H_0 = 50$ m (Lascaratos et al. 1993).

Since the observations show that deep convection below the wind-effected regime is typically nonpenetrative (Schott et al. 1994), the coefficient n can be taken as zero in general. This means that below the depth where wind-driven entrainment plays a role the mixed layer model degenerates into an erosion of the density gradient by the surface buoyancy flux.

The density changes are calculated from the temperature and salinity changes using a local linearized equation of state:

$$\rho = \rho_0[1 - \alpha(T - T_0) + \beta(S - S_0)]. \tag{4}$$

Here α and β are thermal and haline expansion/contraction coefficients and the subscript zero denotes reference values. For the surface temperature and salinity values of the Gulf of Lions in late winter of 13.0°C and 38.4 psu the appropriate values for these coefficients are $\alpha = 2.02 \times 10^{-4}$ °C^{-1} and $\beta = 7.54 \times 10^{-4}$.

3. Surface fluxes

Two types of surface fluxes are required to drive the model. The first are heat and freshwater fluxes, which determine the heating or cooling rate and the buoyancy flux. The second is the work by the wind stress acting on the surface, of which some fraction is made available for deepening the surface-mixed layer. The net heat flux into the ocean consists of the amount of absorbed solar radiation Q_s, the net outgoing longwave radiation Q_b, and the latent and sensible heat fluxes Q_e and Q_h, respectively. Such forcing data are not routinely available from observations. But for a few instances of deep convection activity, meteorological observations over the Gulf of Lions were made from research vessels and the moored platform *Buoée Laboratoire* (Sankey 1973), allowing heat flux estimation based on bulk formula.

For our interannual variability study the only long meteorological time series are standard observations from coastal stations around the Gulf of Lions and, therefore, fluxes are derived through correlations of these observations with the few short flux time series from over the convection regime. As a second approach, the forcing parameters for the winter 1991/92 will be prescribed heat fluxes and wind speed from the French weather forecasting model PERIDOT.

The impact of precipitation on the surface buoyancy flux has been evaluated for the winters 1992/93 and 1993/94, using daily observations from the coastal weather stations, which show a total amount of 127 mm and 62 mm for the period from 15 December to 1 March, respectively. Including these values into the calculation of buoyancy fluxes [Eq. (2)] results in a reduction of 2.7% and 1.9%, respectively, in those winters. Mixed-layer model runs including precipitation data show no significant differences in mixed layer depth or water mass properties when compared to runs without precipitation. The freshwater flux is therefore assumed to be determined only by evaporation, although it might be used as an indicator for mild or strong winters (Bethoux and Tailliez 1994). Without precipitation in the buoyancy flux estimates, there is a close correlation of 0.99 between the time series of heat flux and of buoyancy flux, which means that the variability of the net heat flux is dominated by the latent heat flux, through both components of Eq. (2). Both quantities will be used equivalently in the following.

Results from climatological evaluation of standard heat flux formula (e.g., Bunker 1976; Isemer and Hasse 1987) have been shown to be deficient because they deliver an ~20 W m^{-2} heat gain for the mean fluxes of the entire Mediterranean basin, while the exchange through the Straits of Gibraltar demands an area-average heat loss of 5 W m^{-2} (Gilman and Garrett 1994). This discrepancy has earlier been explained by an underes-

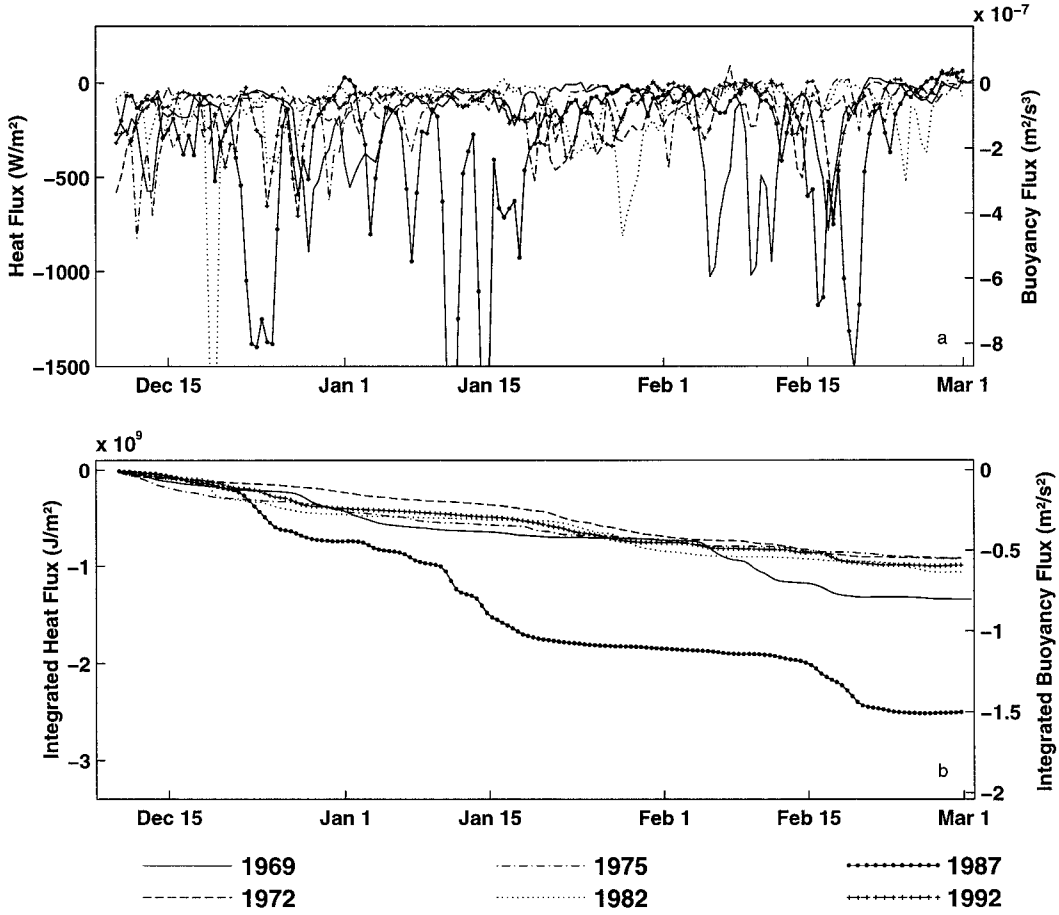

FIG. 2. (a) Daily averaged heat fluxes (left-hand scale) and approximately corresponding buoyancy fluxes (right-hand scale) from the regressions of coastal weather station data for selected winter periods (where known observational programs took place); (b) integrated fluxes.

timation of latent and sensible heat loss (Bunker et al. 1982). Recently Gilman and Garrett (1994) point to the overestimation of shortwave insolation and propose a haze correction during the calm and dry months of May–October that would reduce insolation by the appropriate amount. Further they used a new parameterization for the longwave radiation, derived from direct observations over the Western Mediterranean (Schiano et al. 1993; Bignami et al. 1995), and transfer coefficients given by Smith (1988, 1989) to compute latent and sensible heat fluxes. This leads to higher heat loss through longwave radiation and lower latent and sensible heat loss when compared to standard parameterizations.

a. Coastal weather stations

To estimate heat fluxes and wind forcing during the time period from 1968 to 1994, meteorological parameters recorded at the coastal weather stations Pomègues and Cap Bear (Fig. 1) have been evaluated. These stations have long been recognized as suitable observational points for the meteorological activity over the Western Mediterranean basin (Schott and Leaman 1991). The airmass modification due to air–sea exchange of heat and moisture and the increase in wind speed has been estimated from a fit with time series obtained at an observation platform moored in the center of the convection region from May 1968 to April 1970 (Sankey 1973). These regressions were high for the air and wet-bulb temperatures but lower for the wind speeds, even when selected for quadrants of the preferred mistral/tramontana directions (section a of the appendix). For cloud cover, needed for the radiation calculation, the coastal station data were taken without adjustments.

Heat fluxes are computed for each time step using parameterizations similar to those given in Gilman and Garrett (1994) (section b of the appendix). Latent and sensible heat fluxes are calculated from the coastal station data after the regressions are applied. Examples of the results for total heat and corresponding buoyancy fluxes are shown in Fig. 2 for several winters (where known observational programs took place) of the analysis period.

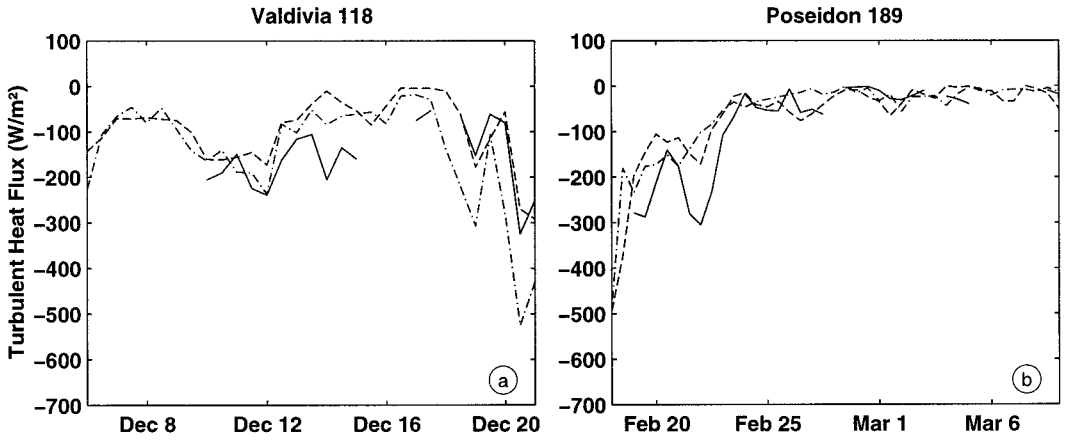

FIG. 3. Half-day averages of the sum of latent and sensible heat flux components from shipboard observations within 100 km of the convection center by (a) RV *Valdivia* in December 1991 and (b) RV *Poseidon* in February/March 1992 (solid) compared with estimates from coastal weather stations (dashed) and PERIDOT model data (dashed–dotted).

b. PERIDOT model

Prescribed heat fluxes and wind speed have been obtained for winter 1991/92 from the French PERIDOT weather forecasting model for the Mediterranean. The data are available on a $1/3° \times 1/4°$ grid as 12-h integrals. Included are fields of the latent and sensible heat fluxes, the solar flux, the downward infrared atmospheric flux, the zonal and meridional components of the wind, and the air temperature. The infrared backradiation flux of the ocean is not provided with the PERIDOT outputs. It has been computed from the relation $Q_{ir} = \varepsilon\sigma T_s^4$ using a mean sea surface temperature of 13.0°C. The net outgoing longwave radiation is therefore given by the difference of Q_{ir} and the downward infrared flux from the PERIDOT data fields.

Comparing PERIDOT model wind speed fields with shipboard observations from RV *Valdivia* in December 1991 and *Poseidon* in February/March 1992, reveals an underestimation in the PERIDOT data of about 40%. Despite this discrepancy in wind speed of the PERIDOT data, it turned out that the latent and sensible heat flux data remained usable as they compare well with direct estimates when the coefficients given by Smith (1988, 1989) are used. Additionally, the model longwave radiation is in good agreement with fluxes computed from the parameterization given by Bignami et al. (1995), although they are much higher as one would expect when using classic formulas. Overall a net difference of 6 W m^{-2} over the winter months from December to March remains between the PERIDOT heat fluxes and the fitted coastal weather station data.

c. Shipboard observations

For the periods during December 1991 and February/March 1992 when shipboard meteorological observations were taken by the Research Vessels *Valdivia* and *Poseidon* within 100 km of the convection center, heat fluxes of both products are compared with the sum of latent and sensible heat fluxes derived from the shipboard data in Fig. 3. There is general agreement for the heat loss maxima on 10–12 and 19–22 December, with larger PERIDOT fluxes during the second period. The moderate phase around 14 December shows significantly larger ship-derived heat losses than either PERIDOT or coastal weather stations, and the ship-derived heat loss maximum of 22 February, during the convection phase is not reproduced in both products.

4. Simulations for winter 1991/92

a. Mixed layer development

The net heat flux from the coastal weather stations and the PERIDOT model for the simulation period from 10 December to 1 March is shown in Fig. 4a. Both show a very similar pattern with several strong events occurring, although they sometimes differ in their peak values. The mixed layer model is integrated with 12-h time steps, using a CTD profile obtained on 10 December at 42°N, 5°E for initialization.

The first mistral event, lasting from 18 to 29 December, shows three peaks of large heat loss ranging from 400 W m^{-2} to 700 W m^{-2}. The mixed layer depth (Fig. 4c) increases to 150 m during this time. This is followed by a calm period of three weeks with a nearly constant mixed layer depth. A second event from 18 to 29 January, with heat losses of 300 W m^{-2} to 400 W m^{-2}, causes a mixed layer deepening to 400 m, thus entraining most of the LIW layer which is then completely mixed by a rather short event taking place around 5 February. Deep convection sets in during the fourth mistral from 14 to 22 February with heat fluxes of up to 700 W m^{-2}. The resulting mixed layer depth varies between 1450 m and 1600 m for the two forcing series.

Integral heat and buoyancy losses over the 82-day simulation period from the coastal weather stations and

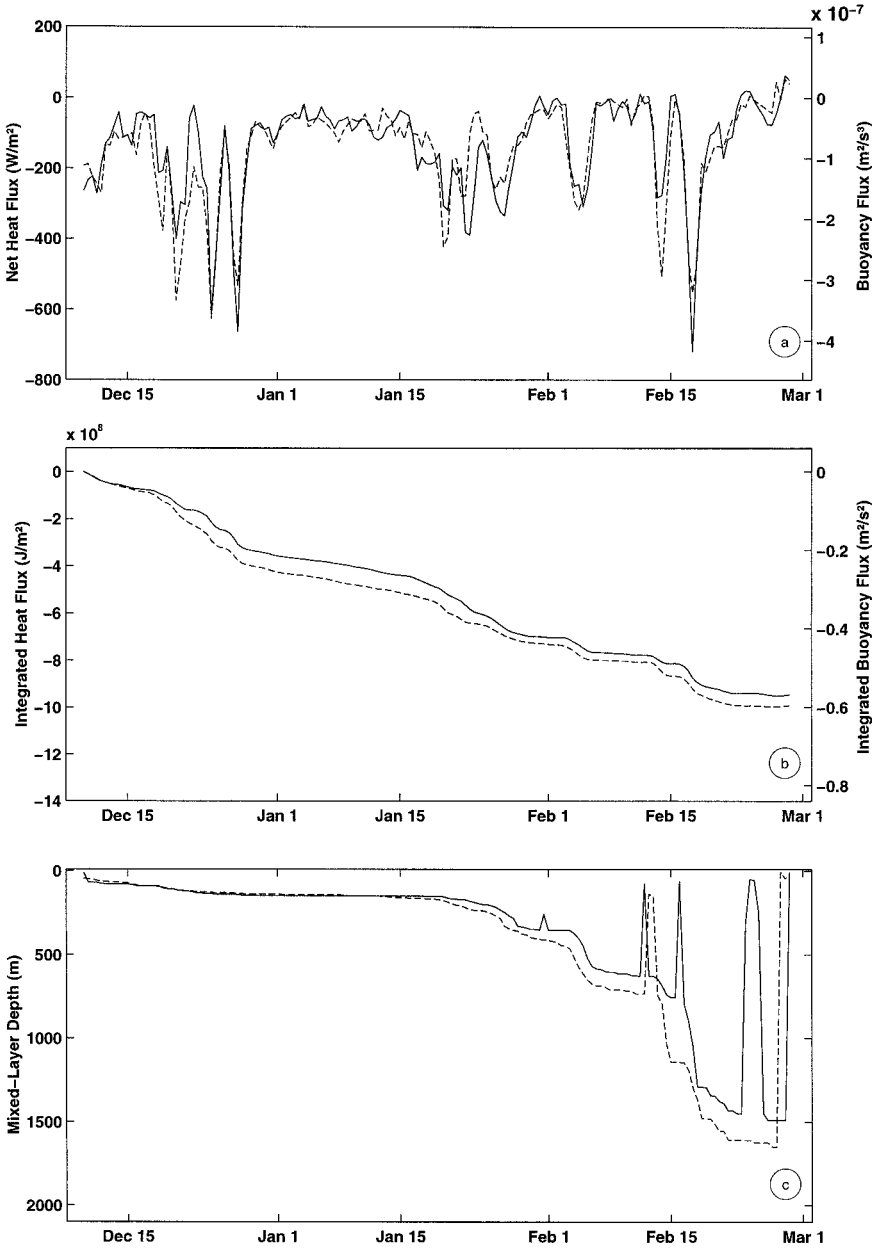

FIG. 4. (a) Half-day averaged total heat flux (left-hand scale) and approximately corresponding buoyancy flux (right-hand scale) in the winter of 1991/92 at 42°N, 5°E as derived from coastal weather stations (solid) and from the PERIDOT model (dashed); (b) same as (a) but seasonal integral; (c) mixed layer depth for model runs with forcing derived from coastal weather stations (solid), and with PERIDOT forcing (dashed).

the PERIDOT model are shown in Fig. 4b. The net heat loss for both runs amounts to about 9.8×10^8 J m^{-2}, which corresponds to a mean heat flux of 138 W m^{-2}, and a total buoyancy flux of 0.59 m^2 s^{-2}.

b. Comparison with observations

A comparison of model results with mooring time series and CTD data is shown in Fig. 5. Two layer averages of temperature and salinity are shown, one over the surface layer (0–150 m), and one over the LIW layer (150–500 m). A depth-weighted average of temperature data, from two moored thermistor strings between 50 m and 730 m (recording at 20 m and 40 m vertical intervals, respectively; available only until 7 February) is shown for comparison.

During the heat loss phase of late December a rapid cooling of the upper layer is observed, with a similar

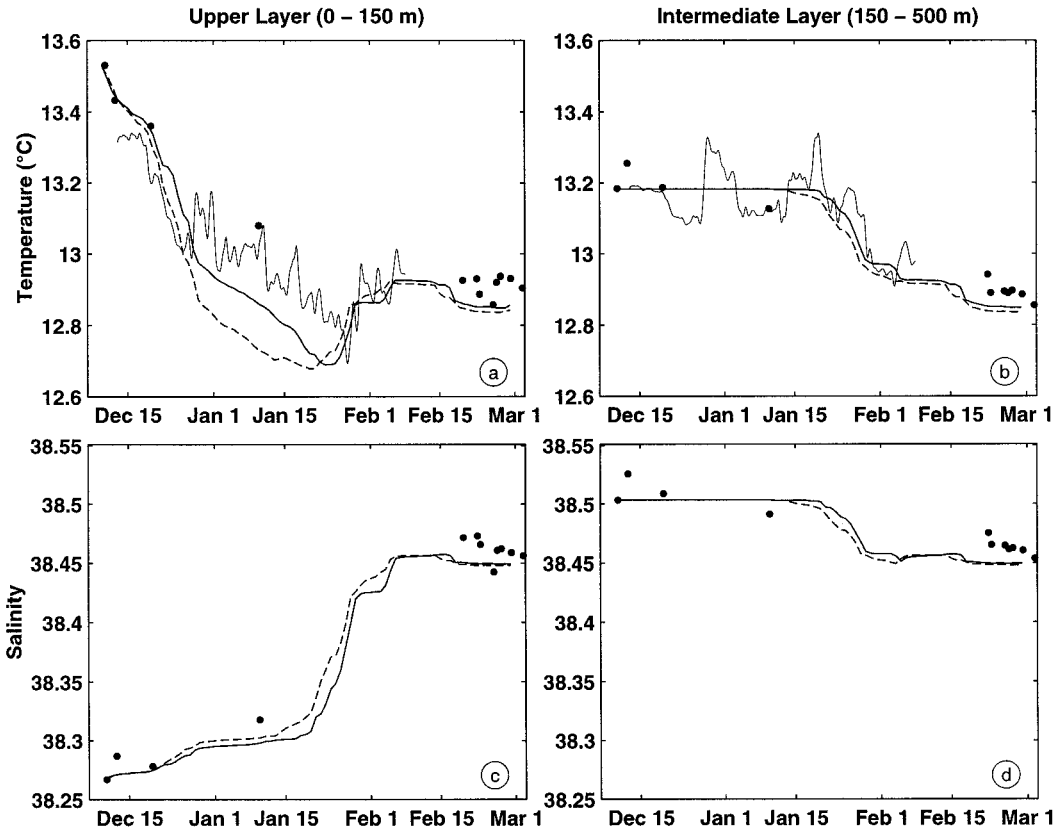

FIG. 5. Layer averages of model mixed layer temperature for 0–150 m (a) and for 150–500 m (b) in the winter of 1991/92 and for salinity (c) and (d). Also shown are layer-averaged temperature records (thin line) from two thermistor strings at mooring A1 between 50 m and 730 m (a) and (b), signatures corresponding to Fig. 4c.

slope in simulations and mooring records. The layer below 150 m is not yet affected. The moderate phase in the first three weeks of January shows a slow cooling of the surface layer at a comparable rate in model and mooring data, although the temperature is lower in the model results. This period is also characterized by advective events, which are of a somewhat transient nature as could be seen in the intermediate layer record where the mooring temperature oscillates around the constant model value. At the end of the moderate cooling phase a minimum temperature of about 12.7°C is reached in the surface layer together with a salinity of 38.3 psu.

In the second heat loss phase of late January the LIW layer gets involved, which results in a warming of the surface layer through the entrainment of warmer intermediate water despite the ongoing cooling at the surface. Correspondingly the surface-layer salinity rapidly increases to 38.45 psu, while the LIW-layer salinity decreases. The comparatively large surface salinity increase during the intermediate-depth preconditioning mixing is a well-known fact, useful for monitoring the extent of the mixed area by surface measurements (Leaman and Schott 1991). To the end of the simulation, the temperature and salinity of the mixed water column drop slightly and lie about 0.03°C and 0.01, respectively, below the observed values.

Comparing actual CTD profiles with the corresponding profiles resulting from the run with coastal weather station forcing (Fig. 6) shows a quite satisfactory agreement with the observed progress of mixing and deep convection during winter 1991/92. Although, as described above, temperature and salinity as well as density are smaller than in the observed profiles. As discussed in Schott et al. (1996) the deep-mixed regime still included a lot of spatial inhomogeneity because it was a case of incomplete mixing; that is, the convective plumes did not have enough time to mix the water as thoroughly as in the case of the stronger 1987 mistral.

5. Interannual variability

In addition to the hydrographic data obtained during the THETIS experiment in the winter of 1991/92, historical data from the time period of 1968–94 (Krahmann 1997) have been analyzed to investigate the interannual variability of late fall conditions in the Gulf of Lions. Regarding the variability and trends of the hydrographic conditions, one has to distinguish between two effects

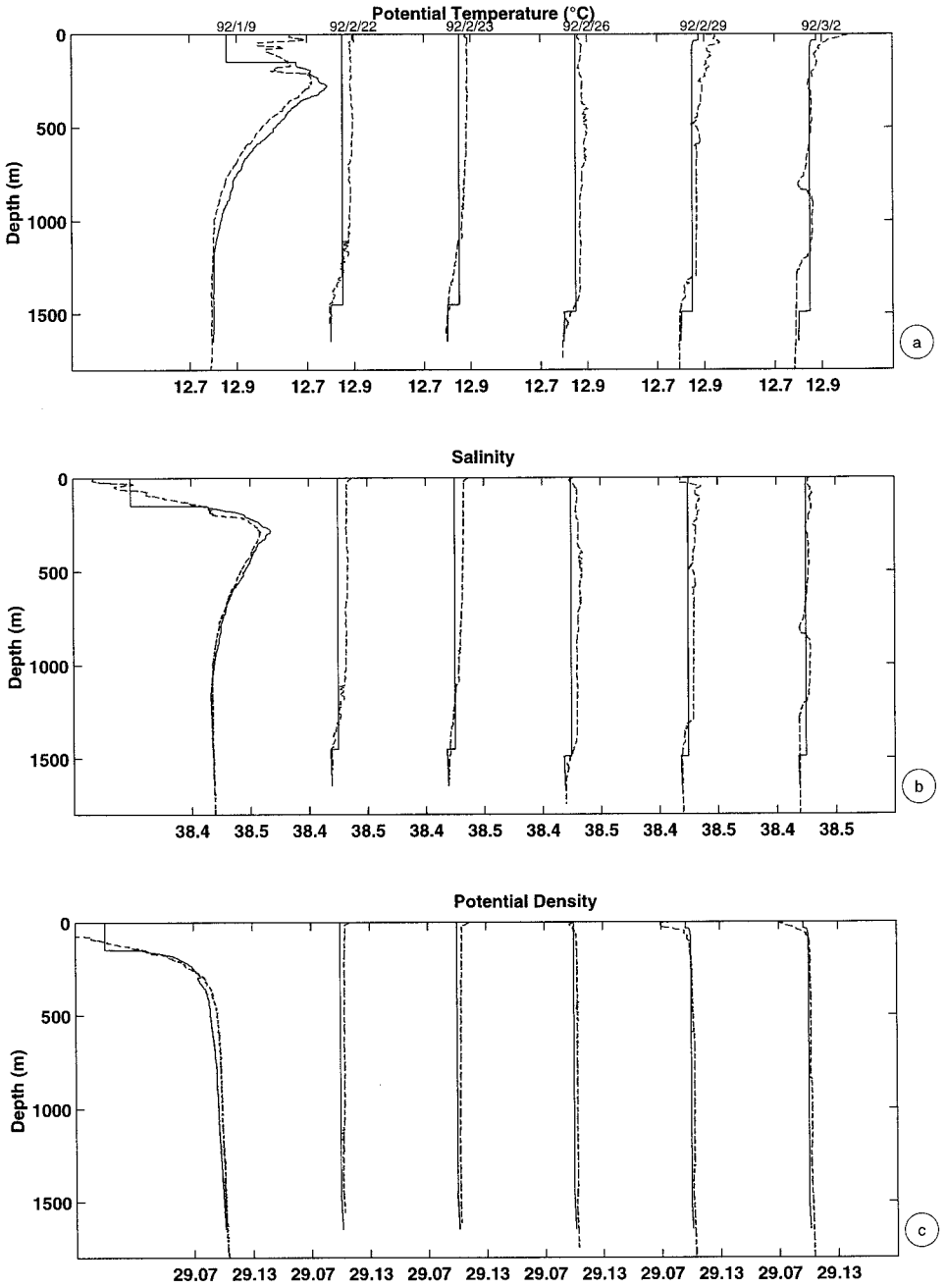

FIG. 6. Temperature (a), salinity (b), and density (c) profiles obtained near mooring A1 during *Le Suroit* (January 1992) and *Poseidon* (February/March 1992) cruises (dashed) and the corresponding model results (solid).

relevant for deep-water formation: density variations altering the amount of buoyancy to be removed from a given profile and therefore changing the mixing depth and density compensated temperature/salinity variations that influence only the properties of the newly formed deep water. However, most of the available profiles have been taken during the convection period itself and only a few profiles could be found for the preconditioning period of November to January during the individual years. Hence, it was not possible to obtain individual initialization profiles for model runs of the different years.

To obtain suitable initial conditions we took all available observations from a square area that roughly coincides with the 90-m depth contour of $\sigma_\theta = 28.8$ (Fig. 1) from November to January and composed three deep

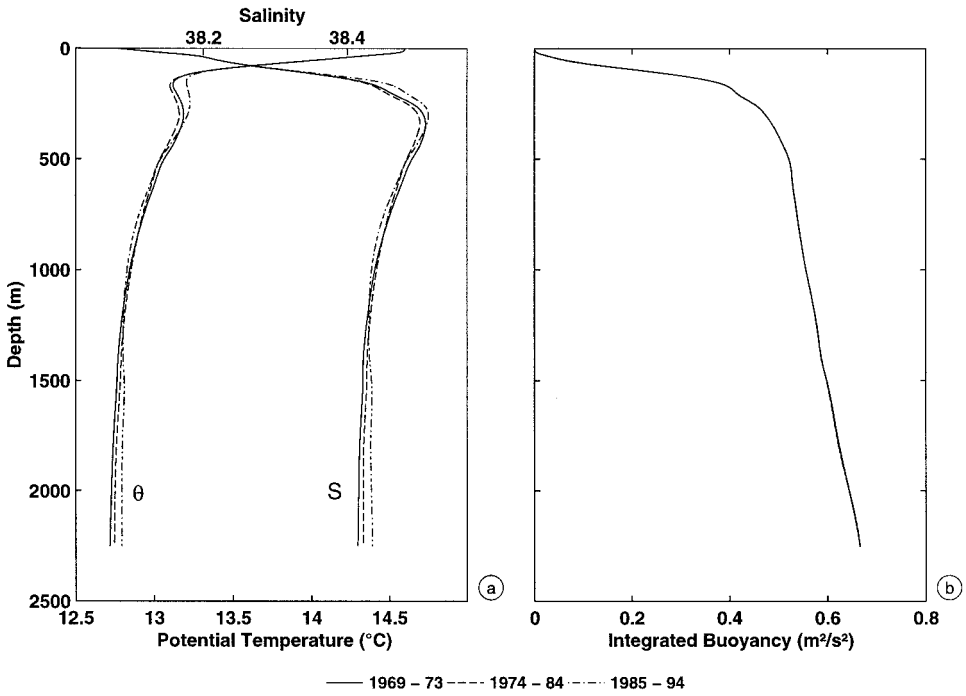

FIG. 7. (a) Climatological temperature and salinity profiles representing the deep water trend that are used to initialize mixed layer model runs; (b) amount of buoyancy that needs to be removed from the climatological profiles to homogenize the water column to a given depth (see text for details).

(below 150 m) mean profiles representing different periods (Fig. 7a). The first profile results from observations of January 1969 and is used as an initial profile for simulations from 1969 to 1973. The second profile consists of data obtained between November 1976 and January 1977 and is used from 1974 to 1984. The THETIS data from November 1991 to January 1992 were averaged to the third profile to represent the years from 1985 to 1994.

As the density variations found in the original profiles were not considered reliable to represent long-term changes and did not show a detectable trend, a constant density profile has been forced by adjusting salinities of the initial profiles at the given temperature slightly through Eq. (4) to obtain the mean density. For the upper 150 m the interannual variability, as well as seasonal changes between November and January, dominate, making it necessary to use averaged climatology data from the box for all observations during November and December.

Interannual variability with amplitudes of ± 0.2°C in temperature and ± 0.05 in salinity has been found for the LIW layer, but it turned out that the variations are compensated in density (Krahmann 1997). The LIW variability would therefore cause a shift to warmer and more saline or colder and less saline newly formed deep water, with the effect decreasing with increasing mixing depth. The effect of the decadal trend of the deep-water properties to higher temperatures (0.03°C/decade) and salinities (0.02/decade) (Leaman and Schott 1991; Rohling and Bryden 1992) is accounted for by the three different profiles.

a. Variability of heat and buoyancy fluxes and modeled mixed layer depths

Heat flux time series derived from the coastal weather station data over the individual winters are shown, for selected years, in Fig. 2a and the integrated fluxes in Fig. 2b. As mentioned above, there is a 0.99 correlation between heat and buoyancy fluxes, and the corresponding buoyancy fluxes are marked on the right-hand side of Fig. 2. Strong mistral bursts are typically of a few days to a week duration, and heat fluxes can exceed 1000 W m^{-2}, as in January 1987, which corresponds to a buoyancy flux of more than 6×10^{-7} m^2 s^{-3}. The integrated heat fluxes between 10 December and 1 March range from 0.8 J m^{-2} in weak mistral years to 2.5 J m^{-2} in the strong convection winter of 1987, corresponding to integral buoyancy fluxes of 0.6 and 1.5 m^2 s^{-2}, respectively.

The buoyancy that needs to be removed from the given preconditioning stratification profiles to homogenize the water column to a given depth is shown in Fig. 7b. All integral buoyancy fluxes exceeding 0.55 m^2 s^{-2} will lead to convection deeper than 1000 m. However, the longer the time period over which this buoyancy flux is distributed, the more advective effects will be important and distort the local balance by bringing in more stratified water, thus preventing convection. On

the other hand, individual events during the middle of winter can contribute 0.3 $m^2 s^{-2}$ over a week, which must then lead to convection when added to the then already advanced surface-mixed layer deepening.

The temporal development of the heat fluxes for the individual years from 1968 to 1994 is shown in Fig. 8a, together with the resulting modeled mixed layer depth in Fig. 8b. The winters of 1980/81 and 1990/91 were omitted due to the lack of meteorological data. In general, it remains until February to remove a sufficient amount of buoyancy from the surface layer for mixing of the weakly stratified deep layers to set in. Extreme situations occurred in the winters of 1984/85 and 1986/87, when very strong mistrals caused convection to the full depth already before mid-January and in the mild winter of 1989/90 when the mixed layer never exceeded 150 m.

Figure 8c shows the maximum mixed layer depth over the simulation period for each winter and the mean net heat and integrated buoyancy fluxes over the winter period (from 10 December to 1 March) are presented in Figs. 8d and 8e, respectively. In addition to the total buoyancy flux, the thermal contribution [according to Eq. (2)] is also shown, which dominates the saline flux by a factor of about 5. The mean heat flux ranges from a low of 65 W m^{-2} in winter 1989/90 to 350 W m^{-2} in winter 1986/87.

The average net heat loss is of about 180 W m^{-2}, with a corresponding buoyancy flux of 0.74 $m^2 s^{-2}$. In several out of the 24 years modeled, when convection did not reach the full water depth, heat and buoyancy fluxes remained below their long-term mean values. Anomalously high heat fluxes occurred during 1985–87 and lower values between 1989 and 1992. The MEDOC 1969 year was one of about average heat flux.

b. Comparison with hydrographic observations

In addition to the model results, observed mixed layer depths during the phase of deep mixing are marked in Fig. 8b (see also Table 1). As regards the individual year results, the convection depths during 1969 and 1970 were slightly deeper than observed. The observed shallow convection depth of only 800 m in 1972 was reproduced well. In 1973, however, the sparse observations available showed homogeneity only to about 500 m, while modeled deep convection extended to the full water depth. The observations available for 1975 and 1982 show convection depths to about 1000 m, while the model results to about 500 m in both cases. Good agreement, as already obvious from the comparison in Fig. 4, is obtained for 1992, although the results from the climatological initialization profile are slightly shallower then those from the actual 1991 profile.

A composite presentation of the observed temperatures and salinities of the deep mixed layer in years when available and the corresponding model results is shown in Fig. 9 and Table 1. The comparison from model results and observations were taken over the same time periods except for winter 1986/87. In this case the model results immediately after the January mistral are shown, which compare rather well with the later observed water mass properties. In mid-February the model values are much colder and saltier, which could be attributed to advective effects during the calm period following the strong mistral. In years of low heat losses and correspondingly low mixed layer depths in winter, the water mass properties of the mixed layer will show high salinities and high temperatures because only part or all of the LIW layer is entrained. Such cases are the late winters of 1972, 1975, and 1982, while strong convection events, such as in 1969, 1970 and 1987, will lead to colder and fresher deep mixed layers.

Differences between the observed and modeled water mass properties and mixed layer depths occur for three reasons: deviation from one-dimensionality, errors in the fluxes, and differences of the actual preconditioning profiles compared to the climatological ones used here. Lateral mixing would result in a reduction of buoyancy flux, depending on the horizontal density gradient in the convection region and could explain shallower observed mixed layer depths than those found in the one-dimensional cases. This would degenerate the other results where good agreement or shallower than observed mixed layer depth has been found. On the other hand, flux errors could account for several hundred meters difference in the final mixed layer depth. As below 500 m the stratification is nearly linear (Fig. 7b), deviations due to flux errors can be estimated as follows: an error of ± 0.01 $m^2 s^{-2}$ in the integrated buoyancy flux (or ± 2.4 W m^{-2} in the mean heat flux) results in a deviation of mixed layer depth of about ± 120 m. Due to this weak stratification of the deep water, the largest differences between observed and modeled mixed layer depths for the winters 1972/73 and 1974/75 of about 750 m (Table 1) can be explained by flux deviations of only ± 0.063 $m^2 s^{-2}$ (or ± 15 W m^{-2}), which correspond to 5%–15% of the total fluxes. Although a constant density profile was used for all model runs, density variations of the initial conditions should be expected in the surface layer. Distributing the buoyancy anomaly of ± 0.063 $m^2 s^{-2}$ to the top 150 m would result in a density anomaly of ± 0.043 kg m^{-3}, with corresponding temperature anomalies of ± 0.21°C or salinity anomalies of ± 0.056. As the differences between modeled and observed temperature and salinity of the newly formed deep water could not be explained by flux errors alone, the uncertainties in the climatological profiles, resulting from variations in the surface layer as well as from the aforementioned variability of the LIW layer, must be considered as the main source of errors for these differences in water mass properties.

6. Summary and conclusions

Forcing time series for deep convection over the Gulf of Lions for 1968–94 were derived by calibrating coastal

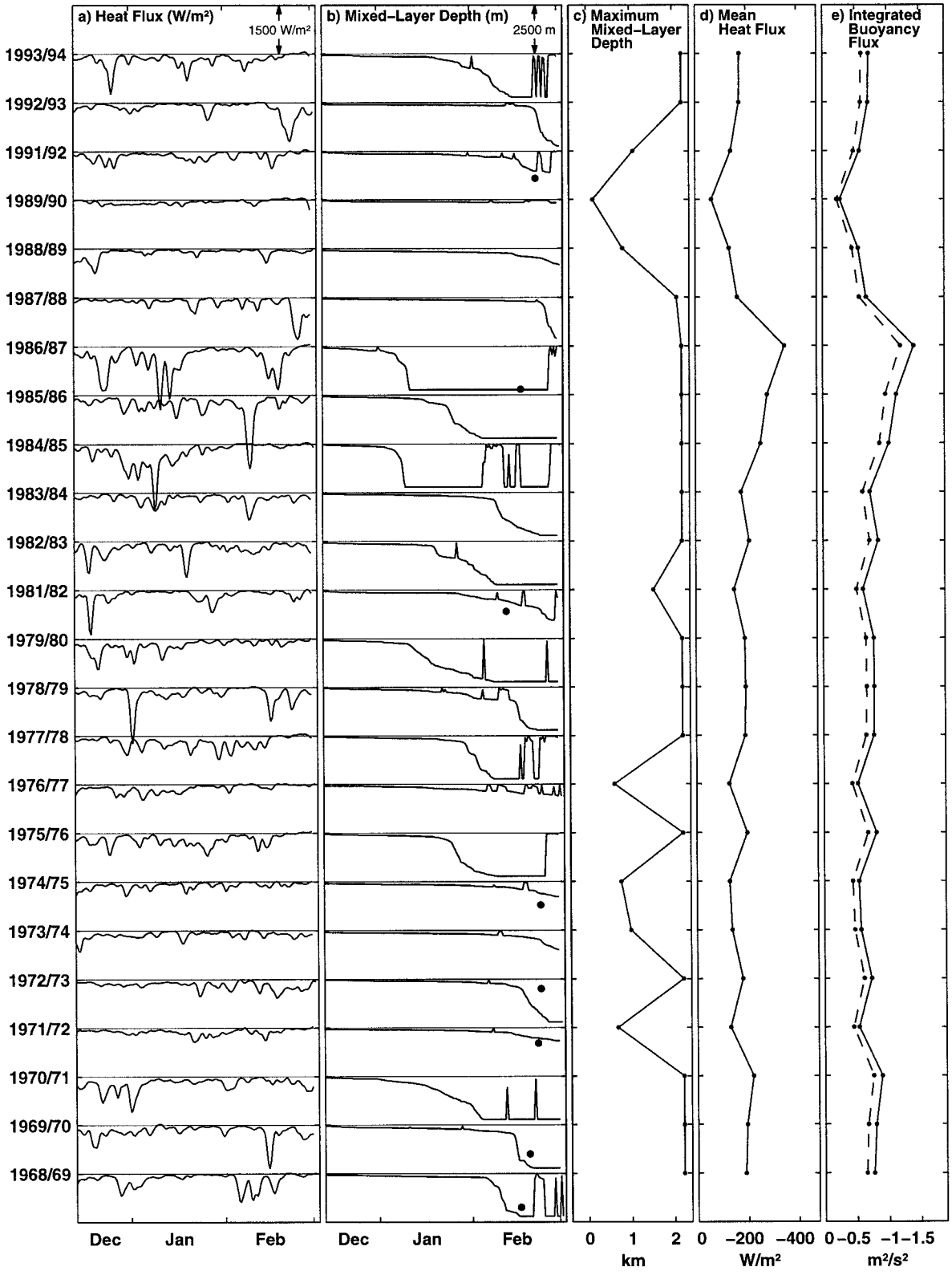

FIG. 8. (a) Heat flux from coastal weather station data; (b) development of mixed layer depth in the model and observed maximum mixed layer depths (dots); (c) maximum mixed layer depth from the model; (d) mean net heat flux of the winter season; (e) integrated total buoyancy flux (solid) and its dominant thermal (dashed); for the individual winters from 1968/69 to 1993/94. The winters of 1980/81 and 1990/91 are missing for the lack of sufficient coastal station observations.

TABLE 1. Mean water mass properties and late-winter mixed layer depths from historical data and the corresponding model results.

Year	February	Number of profiles	Historical data			Mixed layer model		
			θ (°C)	S	H (m)	θ (°C)	S	H (m)
1969	17–26	20	12.793	38.429	1750	12.789	38.437	2200
1970	16–24	16	12.837	38.435	1500	12.823	38.440	1840
1972	23–27	10	12.890	38.439	800	12.902	38.446	540
1973	19–24	3	12.836	38.420	500	12.874	38.449	1220
1975	19–27	26	12.891	38.453	1200	12.875	38.433	440
1982	13–20	15	12.854	38.436	1100	12.889	38.444	570
1987	18–24	9	12.760	38.440	2200	12.760	38.444	2200
1992	20–26	15	12.874	38.459	1400	12.890	38.452	1000

meteorological station data against measurements over the convection site and are then used to drive a mixed layer model for simulating deep convection. The test case was observations from the THETIS experiment in the winter of 1991/92, for which convection depth and deep-mixed water mass properties were well reproduced. In comparison to the calibrated coastal station fluxes for 1991/92 and shipboard flux estimates for brief periods of that winter, heat fluxes from the French weather prediction model PERIDOT were also analyzed, and it was found that despite a discrepancy in the wind speed data the heat fluxes compared reasonably well.

From the 24 years of flux estimates and model simulations, considerable interannual variability was determined. There seemed to be a sequence of years during the past decade with higher than average mean winter heat losses, 1985–87, while in 1989–93 mean heat fluxes were below average.

Interannual variability of mixed layer depths and hydrographic properties, as derived from one-dimensional mixed layer modeling, was compared with observed val-

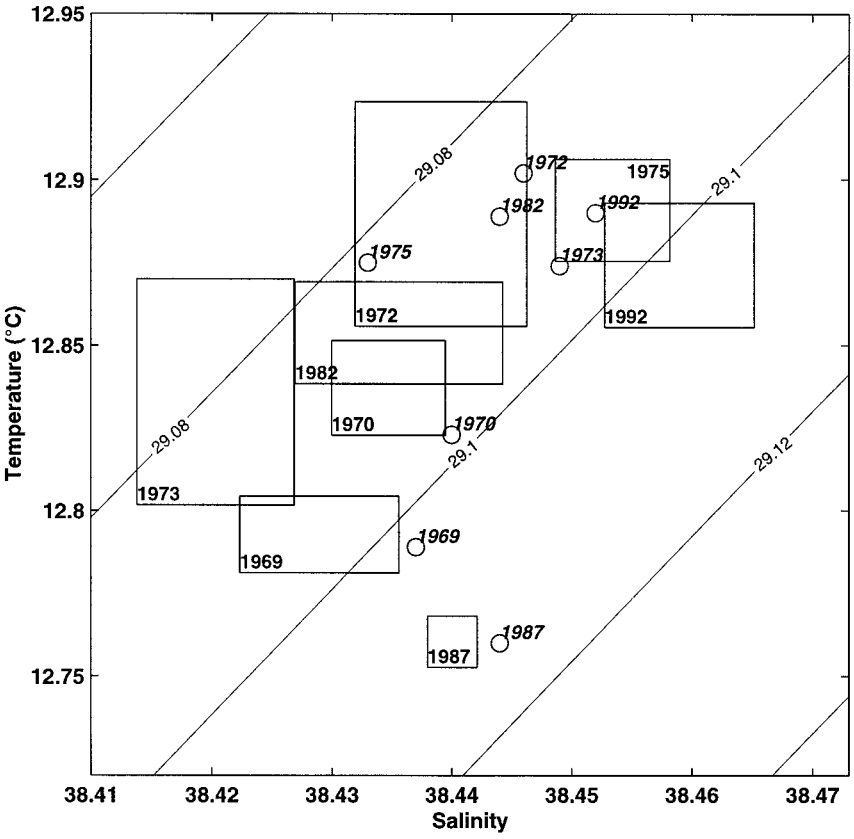

FIG. 9. Temperature–salinity diagram showing characteristics of newly formed deep water from mixed layer model runs compared with hydrographic observations. Observations are shown as boxes determined by the standard deviation of the profiles, and model results are shown as circles.

TABLE 2. Comparison of meteorological parameters, for the winter months of 1968/69 and 1969/70, obtained from coastal weather stations with those from La Bouée Laboratoire (means, standard deviations, and correlation coefficients).

	La Bouée	Pomègues		Cap Bear	
	mean ± std dev	Mean ± std dev	Corr.	Mean ± std dev	Corr.
Air temperature (°C)	11.6 ± 2.9	8.8 ± 3.3	0.84	9.7 ± 3.2	0.78
Wet-bulb temperature (°C)	9.3 ± 3.1	5.9 ± 3.2	0.81	5.7 ± 3.0	0.80
Wind speed (m s^{-1})	12.3 ± 7.1	9.3 ± 5.7	0.53	8.7 ± 6.2	0.51

ues determined from historical hydrographic data. Since data coverage in early winter was not good enough to determine individual year preconditioning temperature and salinity profiles with which to initialize the model runs, mean climatological starting profiles had to be used for each winter. These initial profiles represented the deep trends for increased temperatures and salinities, but were density compensated. Besides the errors in the flux estimates, which due to the week stratification of the deep water may account for differences in mixing depth of several hundred meters when changed by 5%–15%, deviations of the mean from the actual preconditioning profile change the amount of buoyancy that has to be removed to get convection to a certain depth, and also show a signature in the properties of the newly formed deep water.

In light of the expected errors, the simulations agreed reasonably well with the observations, showing that the local heat flux is the dominant effect in driving deep convection in the Gulf of Lions and that, correspondingly, interannual convection variability is closely related to local heat flux variability. Mixed layer depth as well as water mass properties could, to a reasonable extent, be estimated by bulk calculations. Especially for the winter of 1991/92, for which the preconditioning situation is well known and observations have been carried out immediately after the main mistral event, we conclude that the convection depth could be estimated using only the knowledge of surface forcing. The role of lateral mixing becomes increasingly important as time progresses after the mistral event. Hence, the degree of agreement of the one-dimensional model results with the observed mixed layer depth depends on the time between convection and observations.

While for the deep convection variability in the Labrador and Greenland Seas definite decadal variability has been documented (see the review by Dickson et al. 1996), which is closely correlated with the North Atlantic oscillation (NAO) index, such decadal modulation is not apparent from our analysis. Yet Mediterranean precipitation is correlated with the NAO (Hurrel and van Loon 1997). At a high NAO index northern Europe obtains anomalously high winter precipitation while the Mediterranean region obtains below average. Krahmann (1997) found that the upper-layer freshwater budget of the Western Mediterranean is related to the NAO as well as variability of French and Spanish river water discharge. However, these changes appear inferior in determining the local preconditioning situation compared to the variability of ice export into the subpolar convection regimes, which, as occurred during the ''Great Salinity Anomaly'' (Dickson et al. 1988), can effectively shut down a subpolar convection regime by adding substantial buoyancy through surface salinity decrease.

Acknowledgments. G. Krahmann and U. Send contributed to this study through helpful discussions. S. Rahmstorf kindly provided his mixed-layer model code. Funding of the THETIS experiment was through EC/MAST, Contract MASTI-CT90-0008, and of the convection studies was also by the German BMFT, Contract 03R617-3.

APPENDIX

Surface Heat Flux Determination from Coastal Meteorological Observations

a. Heat flux time series from coastal weather stations

Records of meteorological parameters obtained during the winter months at the observation platform *La Bouée Laboratoire*, moored at 42°13.7′N, 5°34.5′E, during the MEDOC 69 and MEDOC 70 experiments are used here to evaluate the modification of air masses advecting from the coast to the center of the convection region. Due to air–sea exchange a conversion from cool continental air to warmer and more humid maritime air occurs, and higher wind speeds have been observed at the platform. Results of the comparison for the winter months of 1968/69 and 1969/70 are summarized in Table 2. Good correlation has been found for air temperature and wet-bulb temperature. Both parameters have been calibrated, using separate linear regressions for both stations, and then averaged. The rms errors result in 1.5°C for the air temperature and 1.7°C for the wet-bulb temperature. However, the scatter found in wind speeds is large, and no useful regression could be applied. Therefore only the mean differences between platform and coastal values have been minimized, which results in an increase of wind speed of 31% for Pomègues and of 41% for Cap Bear values, with an error of 6.6 m s^{-1} after averaging. No correction has been applied to the cloud cover records.

Comparing heat fluxes obtained from the calibrated and averaged time series of the coastal weather stations

with those computed directly from the platform data shows mean differences of 11 W m^{-2} in the latent and sensible heat flux components. These differences result from the nonlinearity induced by the bulk formulas.

b. Heat flux parameterization

The computation of the incoming shortwave radiation is based on Lumb's (1964) formulation:

$$Q_s = Q_0 \sin(\theta)(a + b \sin(\theta))(1 - \alpha), \quad \text{(A1)}$$

where the mean solar flux at the top of the atmosphere Q_0 is taken to be 1368 W m^{-2}, adjusted for seasonally varying earth–sun distance. The solar elevation θ is calculated as a function of time and geographical latitude. In the presence of clouds the coefficients a and b are varied according to Dobson and Smith (1988), depending on the cloud cover fraction. The albedo α is taken from the tables of Payne (1972), which give a typical value of 0.1 for the northwestern Mediterranean in winter. The imposed solar radiation is distributed with depth according to a double exponential relation for moderately clear water of type IA (Paulson and Simpson 1977). Since this formula is derived for hourly computations, it is integrated over each time step in the mixed layer model. The resulting daily averages are in good agreement with the formula of Reed (1977).

For the parameterization of the net longwave radiation recent measurements of radiative fluxes in the Western Mediterranean Sea have led to a new regression algorithm (Bignami et al. 1995):

$$Q_b = \varepsilon\sigma T_s^4 - \sigma T_a^4(0.653 + 0.00535e_a) \times (1 + 0.1762c^2), \quad \text{(A2)}$$

where $\varepsilon = 0.98$ is the emissivity of the ocean surface, σ is the Stefan–Boltzmann constant, and c is the cloud cover; T_a, T_s, and e_a are air temperature, sea surface temperature, and water vapor pressure, respectively.

The latent and sensible heat fluxes are parameterized through the well-known bulk formulas as

$$Q_e = \rho_a L_v c_E(q_s - q_a)U, \quad \text{(A3)}$$

$$Q_h = \rho_a c_p c_H(T_s - T_a)U, \quad \text{(A4)}$$

where ρ_a is the density of moist air, U the wind speed, q_s the saturation specific humidity of air with temperature T_s, q_a the specific humidity of the air, and $c_p = 1004.64$ J kg^{-1} K^{-1} the specific heat capacity. The latent heat of vaporization L_v is calculated as a function of air temperature from Gill (1982). The turbulent exchange coefficients c_E and c_H are taken from tables of Smith (1988, 1989), with $c_H = c_E/1.2$.

REFERENCES

Bethoux, J. P., and D. Tailliez, 1994: Deep-water in the western Mediterranean Sea, yearly climatic signature and enigmatic spreading. *Ocean Processes in Climate Dynamics: Global and Mediterranean Examples*, P. Malanotte-Rizzoli and A. R. Robinson, Eds., Kluwer Academic, 355–369.

Bignami, F., S. Marullo, R. Santoleri, and M. E. Schiano, 1995: Longwave radiation budget in the Mediterranean Sea. *J. Geophys. Res.,* **100**(C2), 2501–2514.

Bunker, A. F., 1976: Computations of surface energy flux and annual air–sea interaction cycles of the North Atlantic Ocean. *Mon. Wea. Rev.,* **104,** 1122–1140.

——, H. Charnock, and R. A. Goldsmith, 1982: A note on the heat balance in the Mediterranean and Red Seas. *J. Mar. Res.,* **40**(Suppl.), 73–84.

Dickson, R. R., J. Meincke, S.-A. Malmberg, and A. J. Lee, 1988: The ''Great Salinity Anomaly'' in the northern North Atlantic 1968–1982. *Progress in Oceanography,* Vol. 20, Pergamon Press, 103–151.

——, J. R. N. Lazier, J. Meincke, P. Rhines, and J. Swift, 1996: Long-term coordinated changes in the convective activity of the North Atlantic. *Progress in Oceanography,* Vol. 38, Pergamon Press, 241–295.

Dobson, F. W., and S. D. Smith, 1988: Bulk models of solar radiation at sea. *Quart. J. Roy. Meteor. Soc.,* **114,** 165–182.

Gascard, J. C., 1973: Vertical motions in a region of deep water formation. *Deep-Sea Res.,* **20,** 1011–1027.

——, 1978: Mediterranean deep water formation, baroclinic instability and oceanic eddies. *Oceanol. Acta,* **1,** 315–330.

Gill, A. E., 1982: *Atmosphere–Ocean Dynamics.* Vol. 30, *Int. Geophys. Ser.,* Academic Press, 662 pp.

Gilman, C., and C. Garrett, 1994: Heat flux parameterization for the Mediterranean Sea: The role of atmospheric aerosols and constraints from the water budget. *J. Geophys. Res.,* **99**(C3), 5119–5234.

Hurrel, J. W., and H. van Loon, 1997: Decadal variations in climate associated with the North Atlantic oscillation. *Climate Change,* **36,** 301–326.

Isemer, H. J., and L. Hasse, 1987: *The Bunker Climate Atlas of the North Atlantic Ocean.* Vol. 2, Springer, 252 pp.

Jones, H., and J. Marshall, 1993: Convection with rotation in a neutral ocean, a study of open ocean deep convection. *J. Phys. Oceanogr.,* **23,** 1009–1039.

Killworth, P. D., 1976: The mixing and spreading phases of MEDOC I. *Progress in Oceanography,* Vol. 7, Pergamon Press, 59–90.

Krahmann, G., 1997: Saisonale und zwischenjährliche Variabilität im westlichen Mittelmeer. Ph.D. dissertation, Institut für Meereskunde, Universität Kiel, 168 pp.

Kraus, E. B., and J. S. Turner, 1967: A one-dimensional model of the seasonal thermocline. Part II: The general theory and its consequences. *Tellus,* **19,** 98–106.

Lascaratos, A., R. G. Williams, and E. Tragou, 1993: A mixed-layer study of the formation of Levantine Intermediate Water. *J. Geophys. Res.,* **98**(C8), 14 739–14 749.

Leaman, K. D., 1994: The formation of western Mediterranean deep water. *Seasonal and Interannual Variability of the Western Mediterranean Sea.* Vol. 46, *Coastal and Estuarine Studies,* P. E. La Violette Ed., Amer. Geophys. Union, 227–248.

——, and F. Schott, 1991: Hydrographic structure of the convection regime in the Gulf of Lions: Winter 1987. *J. Phys. Oceanogr.,* **21,** 573–596.

Lumb, F. E., 1964: The influence of cloud on hourly amounts of total solar radiation at the sea surface. *Quart. J. Roy. Meteor. Soc.,* **90,** 43–56.

Maxworthy, T., and S. Narimousa, 1994: Vortex generation by convection in a rotating fluid. *J. Phys. Oceanogr.,* **24,** 865–887.

MEDOC Group, 1970: Observations of formation of deep water in the Mediterranean Sea, 1969. *Nature,* **227,** 1037–1040.

Millot, C., 1987: Circulation in the Western Mediterranean Sea. *Oceanol. Acta,* **10,** 143–149.

Niiler, P. P., and E. B. Kraus, 1977: One-dimensional models of the upper ocean. *Modeling and Prediction of the Upper Layers of the Ocean,* E. B. Kraus, Ed., Pergamon Press, 143–172.

Paulson, C. A., and J. J. Simpson, 1977: Irradiance measurements in the upper ocean. *J. Phys. Oceanogr.,* **7,** 952–956.

Payne, R. E., 1972: Albedo of the sea surface. *J. Atmos. Sci.,* **29,** 959–970.

Rahmstorf, S., 1991: A zonal-averaged model of the ocean's response to climatic change. *J. Geophys. Res.,* **96,** 6951–6963.

Reed, R. K., 1977: On estimating insolation over the ocean. *J. Phys. Oceanogr.,* **7,** 482–485.

Rohling, E. J., and H. L. Bryden, 1992: Man-induced salinity and temperature increase in western Mediterranean deep water. *J. Geophys. Res.,* **97,** 11 191–11 198.

Sankey, T., 1973: The formation of deep water in the Northwestern Mediterranean. *Progress in Oceanography,* Vol. 6, Pergamon, 159–179.

Schiano, M. E., R. Santoleri, F. Bignami, R. M. Leonardi, S. Marullo, and E. Böhm, 1993: Air–sea interaction measurements in the West Mediterranean Sea during the Tyrrhenian eddy multi-platform observations experiment. *J. Geophys. Res.,* **98**(C2), 2461–2474.

Schott, F., and K. D. Leaman, 1991: Observations with moored acoustic Doppler current profilers in the convection regime in the Golfe du Lion. *J. Phys. Oceanogr.,* **21,** 558–574.

——, M. Visbeck, and U. Send, 1994: Open ocean deep convection, Mediterranean and Greenland Seas. *Ocean Processes in Climate Dynamics: Global and Mediterranean Examples,* P. Malanotte-Rizzoli and A. R. Robinson, Eds., Kluwer Academic, 203–225.

——, ——, ——, J. Fischer, L. Stramma, and Y. Desaubies, 1996: Observations of deep convection in the Gulf of Lions, northern Mediterranean, during the winter of 1991/92. *J. Phys. Oceanogr.,* **26,** 505–524.

Send, U., and J. Marshall, 1995: Integral effects of deep convection. *J. Phys. Oceanogr.,* **25,** 855–872.

Smith, S. D., 1988: Coefficients for sea surface wind stress, heat flux, and wind profiles as a function of wind speed and temperature. *J. Geophys. Res.,* **93**(C12), 15 467–15 472.

——, 1989: Water vapor flux at the sea surface. *Bound.-Layer Meteor.,* **47,** 277–293.

THETIS Group, 1994: Open-ocean deep convection explored in the Mediterranean. *Eos Trans. Amer. Geophys. Union,***75**(19), 217–221.

Visbeck, M., J. Fischer, and F. Schott, 1995: Preconditioning the Greenland Sea for deep convection: Ice formation and ice drift. *J. Geophys. Res.,* **100**(C9), 18 489–18 502.

Voorhis, A., and D. C. Webb, 1970: Large vertical currents observed in a winter sinking region of the northwestern Mediterranean. *Cah. Oceanogr.,* **22**(6), 571–580.